Robust take-off for a quadrotor vehicle

D. Cabecinhas, R. Naldi, L. Marconi, C. Silvestre, R. Cunha

***Abstract*—This paper addresses the problem of robust take-off of a quadrotor UAV (Unmanned Aerial Vehicle) in critical scenarios, such as in presence of sloped terrains and surrounding obstacles. Throughout the maneuver the vehicle is modeled as a hybrid automaton whose states reflect the different dynamic behavior exhibited by the UAV. The original take-off problem is then addressed as the problem of tracking suitable reference signals in order to achieve the desired transitions between different hybrid states of the automaton. Reference trajectories and feedback control laws are derived to explicitly account for uncertainties in both the environment and the vehicle dynamics. Simulation results demonstrate the effectiveness of the proposed solution and highlight the advantages with respect to more standard open-loop strategies, especially for the cases in which the slope of the terrain renders the take-off maneuver more critical to be achieved.**

***Index Terms*—Aerial Robotics, Underactuated Robots, Hybrid Automaton, Optimization**

I. Introduction

Flight control of autonomous Unmanned Aerial Vehicles (UAV) is an active and extensively researched topic, with crucial importance in numerous civilian and military applications [1], [2], [3], [4]. To be truly autonomous, an UAV must perform maneuvers that encompass not only the normal flight conditions, like hover or forward flight, but also the take-off and landing maneuvers, where interaction with the ground occurs. In the critical take-off phase the autopilot controller must provide robustness to uncertainties in both the environment and the dynamical vehicle model. In most of the available literature, automated take-off maneuvers for aerial rotorcraft are performed in a semi open-loop fashion. The maneuvers are achieved by tracking a given trajectory that takes the vehicle to hover, or that descends, at a slow enough rate to hopefully land the aircraft without damage. This is the situation presented in several works, e.g. [5], [6], and [7], where the aspect of ground contact modeling or robustness to environment uncertainties is not dealt with.

Hybrid automata allow to model a complex system in a modular way by collecting simpler dynamical models, each one focusing only on a precise operating mode of the system. They constitute a subset of the larger class of hybrid dynamical systems [8]. Hybrid controllers have been successfully applied for the trajectory tracking of aerial vehicles in different setups, from which we highlight two. In [9], a hybrid controller is designed to fulfill multiple hierarchical objectives and includes a tactical planner, responsible for the higher level behavior of the aircraft, and a trajectory planner, which generates the desired trajectory for each mode. A different hierarchical control architecture for aggressive maneuvering applicable to autonomous helicopters is proposed in [10]. The hybrid controller is based on an automaton whose states represent feasible trajectory primitives. In both papers, different states of the automata correspond to different trajectories and not to different dynamics of the vehicle. Additionally, in the former work, the overall switched system stability analysis is not presented and, in the latter, perfect tracking of the nominal trajectories is assumed.

In this work we target the problem of automatic take-off in critical scenarios where heuristic "open-loop" approaches can not be used to guarantee successful maneuvers and control solutions able to finely steer the vehicle along appropriate trajectories are needed. The prototypical scenario motivating our attempts is sketched in Figure 1. The presence of a left-sided obstacle along with a sloped terrain makes the application of heuristic take-off strategies, for instance based on the application of uncontrolled large vertical thrusts aiming to rapidly detach the vehicle from the ground, inappropriate as leading to hit the obstacle (see the sketch on left of Figure 1). Indeed, as shown on the right of the figure, successful take-off maneuvers necessarily require a first phase in which the vehicle is tilted clockwise by pivoting about the landing gear, followed by a getaway maneuver in which the vehicle slides to the right while keeping the contact with the ground, before definitely taking-off at a safe distance from the obstacle. The accomplishment of this kind of maneuver, in turn, is challenging due to the changes of the dynamics governing the vehicle in the different phases and to the possible uncertainties characterizing the environment and the vehicle. Our goal is precisely to set-up a framework to handle the above scenario and to robustly design successful maneuvers.

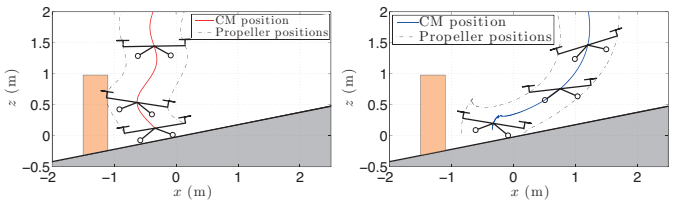

Fig. 1. Left: the quadrotor hits an obstacle if uncontrolled vertical thrusts are applied. Right: a safe take-off maneuver.

The methodology adopted to address this problem borrows from the control framework proposed in [11] and builds upon previous work on ground interactions [12] and interactions with structures in the environment [13]. In this approach, the vehicle is modeled as a *hybrid automaton* where each state corresponds to a different operating condition, where the vehicle is subject to different dynamics, according to the nature of the ground contact. The control methodology presented in the following requires that the current operative mode of the UAV is known. For the specific take-off operation, the operative mode can be retrieved by merging the information deriving from contact or force sensors, to be placed at each extremity of the vehicle's landing gear, with the knowledge of the velocity and the attitude of the system obtained through a standard inertial navigation unit.

Once the hybrid automaton is defined, the take-off control problem is addressed as trajectory generation and tracking control problems. In particular, both the reference signals and the feedback laws for each operating mode are derived considering explicitly the presence of uncertainties. The references are designed such that their practical, and not perfect, tracking ensures that the desired transitions happen, despite the possible presence of parametric or modeling uncertainties. Other approaches to maneuver based motion-planning include [14] and [15], where supervisor hybrid controllers are also used to ensure that a sequence of maneuvers is followed robustly.

The main contribution of this work consists in the explicit design of the hybrid automaton, robust reference maneuvers, and low-level controllers for a quadrotor vehicle. We derive the dynamics for a quadrotor pivoting and/or sliding along a slope and construct a robust hybrid controller, along with the definition of appropriate reference

This work was partially supported by Fundação para a Ciência e a Tecnologia (ISR/IST plurianual funding) and by the project PTDC/EEAACR/72853/2006 HELICIM of the FCT and AIRTICI from AdI.

The work of D. Cabecinhas was supported by a PhD Student Grant from the FCT POCTI program, SFRH / BD / 31439 / 2006.

D. Cabecinhas, C. Silvestre and are with the Department of Electrical Engineering and Computer Science, and Institute for Systems and Robotics, Instituto Superior Técnico, 1049-001 Lisboa, Portugal. {dcabecinhas,cjs,rita}@isr.ist.utl.pt

R. Naldi and L. Marconi are with CASY-DEIS, University of Bologna, Italy. {roberto.naldi,lorenzo.marconi}@unibo.it

trajectories, that allows for fully autonomous robust take-off of the vehicle. Robust reference maneuvers for take-off are obtained as solutions of constrained optimal control problems.

II. Notation

The following mathematical notation is used throughout this work. The expression $g : X \to Y$ indicates that g is a *map* with domain X and codomain Y. Similarly, $h : X \rightrightarrows Y$ denotes a *set-valued map* h with domain X and codomain Y. The *sign* function $\text{sgn}(x) : \mathbb{R} \to \mathbb{R}$ extracts the sign of a real number. For the purposes of this work it is defined as $\text{sgn}(x) = -1$, if x is negative, $\text{sgn}(x) = 1$, if x is positive, and $\text{sgn}(0) = 0$. A *saturation function* is defined as a differential function $\sigma(\cdot) : \mathbb{R} \to \mathbb{R}$ satisfying $|d\sigma(x)/dx| \leq 2$ for all x, $x\sigma(x) > 0$ for all $x \neq 0$, $\sigma(0) = 0$, $\sigma(x) = \text{sgn}(x)$ for $|x| > 1$, and $|x| < |\sigma(x)| < 1$ for $|x| < 1$. For a point $x \in \mathbb{R}^n$, $B_\epsilon(x)$ denotes the ball of radius ϵ centered at x, that is, $B_\epsilon(x) = \{y \in \mathbb{R}^n : \|x - y\| < \epsilon\}$. The symbol $\wedge$ denotes the logical AND operator. The definition of input-to-state stable (ISS) with restrictions for a dynamic system is taken from [16].

III. Quadrotor Hybrid Model

The UAV considered in this paper is a quadrotor aircraft actuated in force, generated by the four propellers. For sake of simplicity, we consider only the "planar dynamics" on the configuration manifold $\mathbb{S}^1 \times \mathbb{R}^2$. The general "spatial dynamics", defined on the configuration manifold $SO(3) \times \mathbb{R}^3$, can be dealt with by properly adapting the presented arguments.

Fig. 2(a) presents a graphical description of the quadrotor geometry and the landing environment. The ground is modeled as a flat surface at an angle β with the horizontal. A body-fixed frame $\{\mathcal{B}\} = \{CM, \vec{j_B}, \vec{k_B}\}$ is attached to the quadrotor's center of mass (CM), with the vector $\vec{k_B}$ pointing upward, along the thrust direction. The inertial frame $\{\mathcal{I}\} = \{O, \vec{j}, \vec{k}\}$ is defined by the vectors $\vec{j}$ and $\vec{k}$ that point North and up, respectively. An additional frame $\{\mathcal{L}\} = \{O, \vec{j_L}, \vec{k_L}\}$ is attached to the origin of $\{\mathcal{I}\}$ and rotated with respect to $\{\mathcal{I}\}$ by an angle β. The angle θ denotes the rotation angle from the inertial frame to the body frame.

The planar model of the quadrotor, illustrated in Fig. 2(b), has two counter-rotating motors for propulsion, generating forces F_1 and F_2, and a landing gear with two points of contact with the ground, denoted by A and B. The distance from the center of mass to each motor and to each contact point are denoted by r and ℓ, respectively. The angle with vertex in CM and subtended by the motor and contact point is denoted by γ. The shorthand $\ell_g = \ell \cos(\gamma)$ is introduced to simplify mathematical expressions. The aerodynamic forces generated by the motors at each of the propellers are represented by F_1 and F_2.

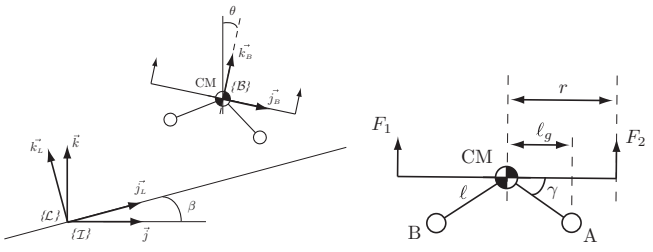

(a) Reference Frames (b) Quadrotor geometry

Fig. 2. Take-off slope and quadrotor

The coordinates of CM in the $\{\mathcal{I}\}$ and $\{\mathcal{L}\}$ reference frames are denoted by (x, z) and (x_L, z_L), respectively, and are related by

$$x_L = x\cos\beta + z\sin\beta,$$
$$z_L = -x\sin\beta + z\cos\beta.$$

The coordinates of the contact point A (α, ζ), expressed in the $\{\mathcal{L}\}$ frame can be written as

$$\alpha = x\cos\beta + z\sin\beta + \ell\cos(\theta + \gamma + \beta),$$
$$\zeta = -x\sin\beta + z\cos\beta - \ell\sin(\theta + \gamma + \beta).$$

Due to the symmetry of the quadrotor, we only consider maneuvers where rotation occurs around the contact point A, resulting in $\theta(t) + \beta \geq 0$, for the operating modes where contact with the ground exists. The symmetric situation is dealt with similarly and will not be discussed in this work.

To simplify computations, the state of the quadrotor is expressed in different coordinate systems, according to its operative mode. When in free flight, the quadrotor state is described by the center of mass coordinates (x, z), the angle θ angle, and their respective derivatives. In situations where contact with the ground occurs, the quadrotor state is completely described by the states α, $\dot{\alpha}$, θ, and $\dot{\theta}$, decoupling the translational motion of the contact point from the rotational motion around the contact point.

In what follows, we adopt the standard *Coulomb friction model* [17] to describe the interaction between the UAV and the terrain. The friction force F_f is bounded in norm by the product of the normal contact force F_N and the friction coefficient μ, as expressed by the constraint $|F_f| \leq \mu F_N$. In case of sliding between the quadrotor and the ground, the magnitude of the friction force is maximum and opposes the movement, resulting in $F_f = -\mu\text{sgn}(\dot{\alpha})F_N$, where

$$F_N = (mg\cos\beta - (F_1 + F_2)\cos(\theta + \beta)), \tag{1}$$

and $\dot{\alpha}$ is the contact point velocity along the slope. In a non-sliding situation, the vehicle will remain at rest until the tangent component of the external forces acting on the vehicle overcomes the friction force limit, $|F_f| \leq \mu F_N$. To allow the quadrotor to start at rest when taking off, and to come to a rest when landing, we require that $\tan\beta < \mu$. Additionally, for simplicity, we consider just one friction coefficient, corresponding to a situation where the kinetic and static coefficients are the same. This nonlinear behavior of the friction force can be modeled in a hybrid automata framework by considering different states for the rest and the sliding situations.

For the development of our quadrotor automaton, we consider five operating modes. These depend on the number of contact points with the ground, and on the relative motion between the vehicle and the ground, which determine different vehicle dynamics. The operating modes are described as follows.

- *Free Flight (FF)* - In this operating mode the quadrotor is in *free flight* and no contact with the landing slope occurs.
- *Take-off-and-Landing (TL and TLs)* - In a *take-off-and-landing* situation, there exists a single contact point between the quadrotor and the ground, depicted as A in Fig. 3(a). The shorthand notation TL denotes the non-sliding situation and TLs the take-off-and-landing mode where sliding exists between the quadrotor and the ground.
- *Landed (LL and LLs)* - In the *landed* operating mode, the landing gear is in full contact with the ground, with both points A and B touching the landing slope, see Fig. 3(b). The shorthand notation LL denotes the non-sliding situation and LLs the landing operative mode were the quadrotor slides on the ground.

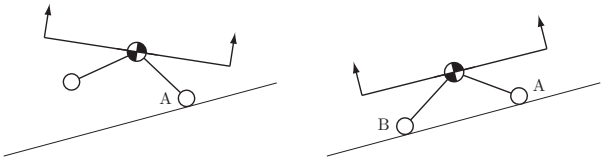

(a) Take-off-and-Landing and Take-off-and-Landing sliding (TL/TLs)

(b) Landed and Landed sliding (LL/LLs)

Fig. 3. Quadrotor operating modes

A. Dynamics of the operating modes

1) Free Flight: In this operating mode the aircraft is airborne. The free flight planar quadrotor is modeled as a rigid body evolving on $\mathrm{SE}(2) = \mathbb{S}^1 \times \mathbb{R}^2$, namely

$$\begin{aligned} m\ddot{x} &= (F_1 + F_2)\sin\theta + \delta_x, \\ m\ddot{z} &= (F_1 + F_2)\cos\theta - mg + \delta_z, \\ J\ddot{\theta} &= (F_1 - F_2)r, \end{aligned} \tag{2}$$

where m and J denote respectively the mass and moment of inertia of the vehicle, g the gravity acceleration, and δ_x and δ_z are exogenous disturbance acting along the lateral and vertical direction. Aerodynamic drag forces are not considered as they are negligible at velocities near the hover condition. To support the employment of the simplified dynamical model proposed above, the Free Flight controller is designed to be robust to external disturbances, which can encompass wind disturbances and modeling uncertainties and errors, up to a given limit.

2) Partial interaction with the ground: In the TL and TLs modes of operation, there is only one contact point of the quadrotor with the ground, as evidenced in Fig. 3(a). The vehicle's motion is restricted to rotation around the contact point A and translation of the contact point along the slope. Recalling that $\alpha \in \mathbb{R}$ is the $\vec{j_L}$ coordinate of the contact point A in the $\{\mathcal{L}\}$ reference frame and that $\theta \in (-\pi, \pi]$ is the rotation angle from the $\{\mathcal{I}\}$ to the $\{\mathcal{B}\}$ reference frame, the generalized forces acting on the vehicle in these operating modes are

$$\begin{aligned} \mathcal{F}_1(F_1, F_2, \dot{\alpha}, \theta) &= (F_1 + F_2)\sin(\theta + \beta) \\ &\quad - \mu\mathrm{sgn}(\dot{\alpha})(mg\cos\beta - (F_1 + F_2)\cos(\theta + \beta)), \\ \mathcal{F}_2(F_1, F_2) &= F_1(r + \ell_g) - F_2(r - \ell_g). \end{aligned}$$

The Lagrangian function of the system in the TL and TLs modes, considering the kinetic and potential energies, is

$$\begin{aligned} \mathcal{L} &= \tfrac{1}{2}m(\dot{x}^2 + \dot{z}^2) + \tfrac{1}{2}J\dot{\theta}^2 - mgz \\ &= \tfrac{1}{2}m(\dot{\alpha}^2 + \dot{\theta}^2\ell^2 + 2\dot{\alpha}\dot{\theta}\ell\sin(\theta + \beta + \gamma)) \\ &\quad + \tfrac{1}{2}J\dot{\theta}^2 - mg(\alpha\sin\beta + \ell\sin(\theta + \gamma)). \end{aligned}$$

In order to simplify the design of controller for the dynamic system we define two virtual controls, F_α and F_θ, related to the real actuations by

$$\begin{pmatrix} F_\alpha \\ F_\theta \end{pmatrix} = L(\theta)^{-1}G(\theta)M \begin{pmatrix} F_1 \\ F_2 \end{pmatrix} \tag{3}$$

where M, $G(\theta)$, and $L(\theta)$ are given by

$$\begin{aligned} M &= \begin{pmatrix} 1 & 1 \\ r + \ell_g & \ell_g - r \end{pmatrix}, \\ G(\theta) &= \begin{pmatrix} \sin(\theta + \beta) + \mu\mathrm{sgn}(\dot{\alpha})\cos(\theta + \beta) & 0 \\ 0 & 1 \end{pmatrix}, \\ L(\theta) &= m\begin{pmatrix} 1 & \ell\sin(\theta + \gamma + \beta) \\ \ell\sin(\theta + \gamma + \beta) & \ell^2 + J/m \end{pmatrix}, \end{aligned}$$

respectively. This input transformation is always defined, since $L(\theta)$ is invertible for all θ, and results on the following dynamics, after solving the Lagrangian equations defining the system,

$$\ddot{\alpha} = F_\alpha + h_\alpha(\theta, \dot{\theta}, \dot{\alpha}, \mu), \quad \ddot{\theta} = F_\theta + h_\theta(\theta, \dot{\theta}, \dot{\alpha}, \mu), \tag{4}$$

where

$$\begin{aligned} h_\alpha(\theta, \dot{\theta}, \dot{\alpha}, \mu) &= \frac{1}{J + m\ell^2\cos^2(\beta + \gamma + \theta)}\Big(- g(J + m\ell^2)\cdot \\ &\quad \cdot(\mu\cos\beta\mathrm{sgn}(\dot{\alpha}) + \sin\beta) + gm\ell^2\cos(\gamma + \theta)\sin(\gamma + \theta + \beta) \\ &\quad - \ell(J + m\ell^2)\cos(\gamma + \theta + \beta)\dot{\theta}^2\Big), \end{aligned} \tag{5}$$

$$\begin{aligned} h_\theta(\theta, \dot{\theta}, \dot{\alpha}, \mu) &= \frac{m\ell}{J + m\ell^2\cos^2(\beta + \gamma + \theta)}\Big(\cos(\gamma + \theta + \beta)\cdot \\ &\cdot(-g\cos\beta + \ell\sin(\gamma + \theta + \beta)\dot{\theta}^2) + g\mu\cos\beta\sin(\gamma + \theta + \beta)\mathrm{sgn}(\dot{\alpha})\Big). \end{aligned} \tag{6}$$

The input transformation (3) is invertible if and only if the matrix $G(\theta)$ is non-singular, as matrix M is full rank. That is, the original forces F_1 and F_2 are recoverable from F_α and F_θ if

$$\sin(\theta + \beta) + \mu\mathrm{sgn}(\dot{\alpha})\cos(\theta + \beta) \neq 0.$$

Note that the inverse transformation depends on a number of physical parameters, and in particular on μ which is typically uncertain.

The dynamics (4) apply only to a quadrotor *sliding* along the slope. In the *take-off and landing* operating mode, the vehicle is in a non-sliding situation. The α position is constant and the dynamic system is reduced to the angular component of (4) with $\dot{\alpha} = 0$, resulting in

$$\ddot{\theta} = F_\theta + h_\theta(\theta, \dot{\theta}, 0, \mu). \tag{7}$$

Equations (4) and (7) describe a 4-state dynamical model for the vehicle. The coordinates of the center of mass and its derivatives are uniquely defined by the states α, $\dot{\alpha}$, θ, and $\dot{\theta}$.

3) Complete interaction with the ground: In the LL and LLs operating modes, the vehicle is completely landed and only the ground contact friction affects the motion of the vehicle. As in these configurations it is impossible to generate forces along the $\vec{j_L}$ axis of the $\{\mathcal{L}\}$ frame, the only effect of the controls F_1, F_2 is to reduce the normal force F_N, consequently reducing the friction force F_f. The dynamic model for the LLs operating mode is completely described by the dynamical system

$$m\ddot{\alpha} = -mg\sin\beta - \mu\mathrm{sgn}(\dot{\alpha})F_N, \quad \dot{\theta} = 0, \tag{8}$$

with F_N given by (1). When in the LL operating mode, this reduces to

$$\dot{\alpha} = 0, \quad \dot{\theta} = 0, \tag{9}$$

and the vehicle's state remains constant. In these operative modes, and in order to prevent physically impossible transitions from LL to FF by employing discontinuous forces, we extend the system input with two integrators, where (v_1, v_2) are the residual control inputs

$$\dot{F}_1(t) = v_1(t)\,, \qquad \dot{F}_2(t) = v_2(t). \tag{10}$$

B. Hybrid model of the overall dynamics

A description of the overall dynamics is obtained by means of a *hybrid automaton* whose states correspond to the operating modes described above. A hybrid automaton is identified by the following objects, instanced here for the specific case of the planar quadrotor.

1) Operating Modes: The quadrotor automaton comprises the set $\mathcal{Q}$ of *operating modes*, denoted by $\mathcal{Q} = \{LL,\ LLs,\ TL,\ TLs,\ FF\}$.

2) Domain map: The state of the system $\xi \in \mathbb{R}^6$ is described by either $(x, \dot{x}, z, \dot{z}, \theta, \dot{\theta})$ or $(\alpha, \dot{\alpha}, z_L, \dot{z}_L, \theta, \dot{\theta})$. When the UAV is in contact with the ground (LL, LLs, TL, and TLs operating modes), the preferred reference frame and the state $\xi = (x, \dot{x}, z, \dot{z}, \theta, \dot{\theta})$ are the $\{\mathcal{L}\}$ frame, yielding $\xi = (\alpha, \dot{\alpha}, z_L, \dot{z}_L, \theta, \dot{\theta})$, while the $\{\mathcal{I}\}$ frame is preferred for the free flight mode. The inputs F_1 and F_2, which correspond to the forces generated by the propellers, are bounded by a minimum and maximum value, leading to the definition of the input domain $U \subset \mathbb{R}^2$ as the compact interval $U = [F_{\min}, F_{\max}] \times [F_{\min}, F_{\max}]$. The domain mapping $\mathcal{D} : \mathcal{Q} \rightrightarrows \mathbb{R}^6 \times \mathbb{R}^2$ defines, for each operating mode, the set of values that the state ξ and the control input u may take.

3) Flow map: The flow map $f : \mathcal{Q} \times \mathbb{R}^6 \times \mathbb{R}^2 \to \mathbb{R}^6$ describes for each operating mode $q \in \{LL, LLs, TL, TLs, FF\}$ the evolution of the state variables. In each operating mode q we have the dynamic system $\dot{\xi} = f(q, \xi, u)$, where each function $f(q, \xi, u)$ is derived from the differential equations (2), (4), (7), (8), and (9).

4) Edges: The set of edges $\mathcal{E} \subset \mathcal{Q} \times \mathcal{Q}$ includes all the pairs (q_1, q_2) such that a transition between the modes q_1 and q_2 is possible, for some combination of state and actuation. For the take-off and landing procedure, we consider the transitions depicted in Fig. 4. We do not consider direct edges linking LL to FF or FF to LL as these transitions are not considered in the following design of the take-off and landing maneuvers due to possible robustness issues. Observe also that they can be equivalently obtained by passing instantaneously trough the intermediate operative modes TL and TLs.

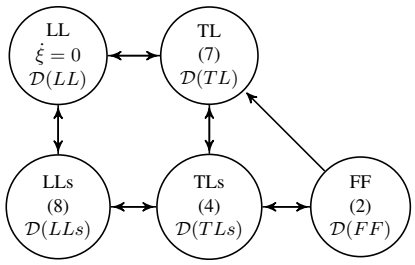

Fig. 4. Planar quadrotor hybrid automaton

5) Guard mapping: The set-valued guard mapping $\mathcal{G} : \mathcal{E} \rightrightarrows \mathbb{R}^6 \times \mathbb{R}^2$ determines, for each edge $(q_1, q_2) \in \mathcal{E}$, the set $\mathcal{G}(\{q_1, q_2\})$ to which the quadrotor state ξ and inputs F_1, F_2, must belong so that a transition from q_1 to q_2 can occur. There are three main groups of transitions to consider for the take-off and landing procedures. The transition from two contact points (LL and LLs operating modes) to one contact point (TL, TLs) is governed by the sign of the torque F_τ at point A,

$$F_\tau(\theta, F_1, F_2) = (F_1 + F_2) l_g + (F_1 - F_2) r - mg\ell \cos(\theta + \gamma),$$

and the inverse transition depends on the angle of the vehicle with the slope, $\theta + \beta$, and also on sign of F_τ. The operating mode transitions between free flight and the TLs mode depend on the force perpendicular to the slope $F_\perp$,

$$F_\perp(\theta, F_1, F_2) = (F_1 + F_2) \cos(\theta + \beta) - mg \cos\beta,$$

and the height of the quadrotor relative to the ground. Lastly, the transitions between the *at rest* and the *sliding* modes are governed by the relation between the force along the slope at the contact point $(F_\alpha + h_\alpha)$, the perpendicular force $F_\perp$, and the vehicle's velocity along the slope $\dot{\alpha}$, according to the Coulomb friction model. The function

$$F_{\text{slide}}(\theta, \dot{\theta}, F_1, F_2, \mu) = |F_\alpha(\theta, \dot{\theta}, \mu, F_1, F_2) + h_\alpha(\theta, \dot{\theta}, 0, \mu)| - \mu \frac{mg \cos\beta}{m \cos^2(\theta + \beta + \gamma)} + \mu \frac{(F_1 + F_2)\cos(\theta + \beta)}{m \cos^2(\theta + \beta + \gamma)}$$

encapsulates these relations. A transition from a non-sliding mode to a *sliding* mode occurs for $F_{\text{slide}} > 0$, whereas a reverse transition happens when the velocity along the slope reaches zero and $F_{\text{slide}} < 0$. In the landed operating mode, this function is reduced to

$$F_{\text{slide}}(-\beta, 0, F_1, F_2, \mu) = mg \sin\beta - \mu(mg \cos\beta - (F_1 + F_2)).$$

6) Reset maps: For each $(q_1, q_2) \in \mathcal{E}$ and $(\xi, u) \in \mathcal{G}(\{q_1, q_2\})$, the reset map $\mathcal{R} : \mathcal{E} \times \mathbb{R}^6 \times \mathbb{R}^2 \to \mathbb{R}^6$ identifies the jump of the state variable ξ during the operating mode transition from q_1 to q_2. The jumps in the state reflect instantaneous changes which are caused by the collisions of the contact points with the landing slope. In the take-off maneuver the nominal transitions do not involve impact with the ground and thus all the reset maps are trivially the identity maps.

IV. The Control Problem

A. Robust Control Strategy and Architecture

With the hybrid automaton in hand, the problem of performing a take-off maneuver can be reformulated as a problem of changing the operative mode q from the initial landed configuration LL to the final free-flight mode FF, by passing through intermediate states like TL and TLs. The problem requires control policies achieving a transition to a desired operative mode robustly with respect to uncertainties in the model and environment parameters. At the same time, all transitions leading to an undesired final configuration must be avoided. Motivated by the scenario in Figure 1, the targeted take-off maneuver involves the transition between the following sequence of hybrid states $LL \to TL \to TLs \to FF$. In all the above sequence the state LLs is regarded as a unideal state to be avoided in the course of the maneuver. Indeed, the system in the LLs mode lacks of control authority in the lateral direction, rendering LLs an undesired state when targeting robust maneuvers.

Inspired by the general framework proposed in [11], the control problem is divided into two different steps. The first step amounts to computing, for each of the three desired transitions ($LL \to TL$, $TL \to TLs$ and $TLs \to FF$) and for the final free flight mode, reference trajectories for both the states ξ and the inputs u of the system, jointly denoted as *reference maneuvers*, whose tracking guarantees that the desired transition takes place. A key issue is to generate *robust reference maneuvers* whose practical, and not perfect, tracking guarantees the desired transition while preventing the system to entering undesired modes. In the proposed framework robustness is quantified in terms of a design parameter $\epsilon > 0$ that roughly expresses how far the actual motion of the system's state and input can be with respect to the reference maneuver in order to have the desired transition effectively imposed.

The second step consists of designing feedback control laws guaranteeing that, for the given reference maneuvers, the tracking error (both in the state and in the input) is upper bounded by ϵ so that the planned transition is enforced. To this purpose the proposed control architecture (sketched in Figure 5) is constituted by a set of low level controllers, associated to the specific operative modes in which the vehicle operates, and a supervisor. The role of the latter is to enable the appropriate low level controller, and to feed it with the appropriate robust reference maneuver. The key requirement behind the design of the low level controllers is to guarantee that, under appropriate restrictions on the initial conditions and bound on the parametric/exogenous disturbances, the tracking error is upper bounded by ϵ.

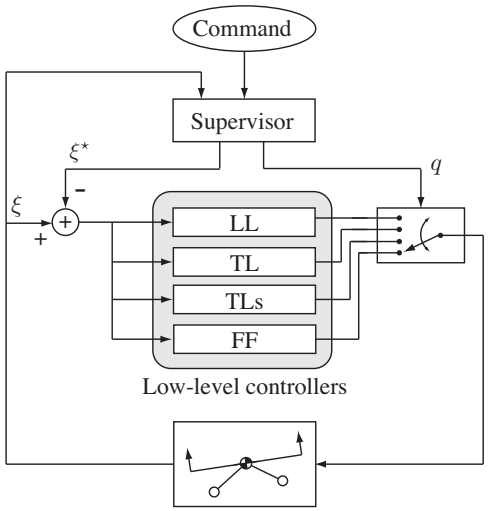

Fig. 5. Proposed control architecture, featuring the supervisor and low-level controllers.

B. Design of Robust Reference Maneuvers

The computation of robust reference maneuvers regarding a desired transition between the generic hybrid states $q_1^\star$ and $q_2^\star$ involves a problem of nominal inversion of the system dynamics in the operative mode $q_1^\star$ that can be approached in different ways. In this paper, the problem is formulated as an optimal problem and a numerical tool is used for the practical computation of the reference maneuvers (see Section V for details on the adopted numerical tool). With $\dot{\xi} = f(q_1^\star, \xi, u, \rho)$ the model of the system in the operative mode $q_1^\star$ with parametric uncertainty ρ, the optimal problem is formulated, in general terms, as follow:

$$\min_{u^\star(t), \xi^\star(t), t_f} \; t_f + \int_{t_0}^{t_f} \|u^\star(\tau)\|^2 d\tau$$

subject to

$$(a)\; \dot{\xi}^\star = f(q_1^\star, \xi^\star(t), u^\star(t), \rho_0)\,, \quad \xi^\star(t_0) = \xi_0^\star\,,\; t \in [t_0, t_f]$$
$$(b)\; u^\star(t) \in \mathcal{U}\,, \quad t \in [t_0, t_f]$$
$$(c)\; \chi_\epsilon(q_1^\star, q_2^\star, \xi^\star(t), u^\star(t)) \leq 0\,, \quad t \in [t_0, t_f]$$
$$(d)\; \Psi_\epsilon(q_1^\star, q_2^\star, \xi^\star(t_f), u^\star(t_f)) \leq 0\,.$$

In the previous formulation the index cost is clearly shaped in order to trade-off the time needed to accomplish the desired maneuver (note that the final time t_f is a degree-of-freedom) and the required control energy, which depends on the magnitude of the forces generated by the quadrotor propellers. The constraints (a) and (b) force the solution to be functionally controllable for the nominal system in the operative mode $q_1^\star$ and to fulfill actuator limitations characterizing the real system. In this respect it is worth noting that nominal value ρ_0 of the uncertainty ρ is used in (a), namely that an inversion of the *nominal* system is necessarily targeted. A special role in (a) is played by the initial condition $\xi_0^\star$ that is a degree-of-freedom to be played in order to properly concatenate consecutive reference maneuvers in the sequence of transitions. Finally, the functions $\chi_\epsilon(\cdot)$ and $\Psi_\epsilon(\cdot)$ in (c) and (d) must be properly specified in order to have the maneuver $(\xi^\star(t), u^\star(t))$ solution of the optimal problem accomplishing the desired transition task. In this respect, by bearing Section IV-A and the meaning of the parameter ϵ in the definition of robust transition maneuver, the function $\chi_\epsilon(\cdot)$ must be specified in a way that maneuvers $(\xi^\star(t), u^\star(t))$ fulfilling (c) are necessarily ϵ-far from any undesired guard set (i.e. guard set different from $\mathcal{G}(q_1^\star, q_2^\star)$), so that switches to undesired hybrid modes are avoided. In a more precise way $\chi_\epsilon(\cdot)$ must be such that any $(\xi^\star(t), u^\star(t))$ fulfilling (c) necessarily satisfies

$$(x^\star(t), u^\star(t)) \bigcap \left(\bigcup_{(q_1^\star, q_2) \in \mathcal{E}\,, q_2 \neq q_2^\star} \mathcal{G}(q_1^\star, q_2) + \mathcal{B}_\epsilon \right) = \emptyset$$

for all $t \in [t_0, t_f]$. Furthermore, possible other path constraints, such as the avoidance of obstacles nearby the take-off area, can be taken into account in the definition of $\chi_\epsilon(\cdot)$ by defining forbidden regions in the x-z plane.

As far as the constraint (d) is concerned, the function $\Psi_\epsilon(\cdot)$ must be properly shaped in a way that any maneuver $(\xi^\star(t), u^\star(t))$ fulfilling (d) at time t_f is necessarily ϵ-inside the guard set $\mathcal{G}(q_1^\star, q_2^\star)$, namely

$$(\xi^\star(t_f), u^\star(t_f)) + \mathcal{B}_\epsilon \subset \mathcal{G}(q_1^\star, q_2^\star)\,.$$

In this way any actual maneuver $(\xi(t), u(t))$ that is ϵ-close to $(\xi^\star(t), u^\star(t))$ necessarily enters, at a time upper bounded by t_f, the set $\mathcal{G}(q_1^\star, q_2^\star)$ so that the desired transition is enforced.

It is worth noting that possible uncertainties characterizing the environment (such as the slope of the terrain, the friction coefficient, the position of nearby obstacles, etc.) affect, in general, the definition of the guard sets and thus the design of $\chi_\epsilon(\cdot)$ and $\Psi_\epsilon(\cdot)$. In this respect a crucial issue in the specification of $\chi_\epsilon(\cdot)$ and $\Psi_\epsilon(\cdot)$ is to adopt the *a priori* knowledge about the uncertainties (such as compact sets where they range) so that the fulfillment of (c) and (d) leads to the desired transition robustly.

The above optimization problem is solved for each of the transition maneuvers $LL \to TL$, $TL \to TLs$, and $TLs \to FF$, with the constraints derived keeping in mind the description of the hybrid automaton presented in Section III. In order keep the analysis at a tractable level, we only consider uncertainties in the ground friction coefficient μ, which affects the modes where contact with the ground exists, and no uncertainties in the slope β of the landing surface. About the value of μ we assume to know only upper and lower bounds denoted by μ^U and μ^L, respectively, and we let $\mu_0 \in [\mu^L, \mu^U]$ be the nominal value of μ.

C. Design of low-level controllers

In this part we address the design of the local controllers in each operating mode involved in the take-off maneuver. The goal of the controller is guarantee that, under appropriate restrictions on the initial conditions and of the exogenous disturbances, the specific reference maneuver is tracked with an error that is upper bounded by ϵ so that the desired transition takes place.

1) Low level controller in the LL mode: With $u^\star(t) = (v_1^\star(t), v_2^\star(t)) : [t_0, t_f] \to \mathbb{R}^2$ and $\xi^\star(t) = (F_1^\star(t), F_2^\star(t)) : [t_0, t_f] \to \mathbb{R}^2$ a robust reference maneuver solution of the optimal problem in Section IV, for some $\epsilon > 0$ and dynamics (9) and (10), the control law is simply chosen as

$$v_1 = -k(F_1 - F_1^\star) + v_1^\star\,, \quad v_2 = -k(F_2 - F_2^\star) + v_2^\star \qquad (11)$$

where k is a positive design parameter.

2) Low level controller in the TL mode: With $u^\star(t) = (F_1^\star(t), F_2^\star(t)) : [t_0, t_f] \to \mathbb{R}^2$ and $\xi^\star(t) = (\theta^\star(t), \dot{\theta}^\star(t)) : [t_0, t_f] \to \mathbb{R}^2$ a robust reference maneuver solution of the optimal problem in Section IV-B, applied to the TL mode dynamics (7), for some $\epsilon > 0$, we define (see (3))

$$F_\theta^\star(t) = \begin{pmatrix} 0 & 1 \end{pmatrix} L(\theta^\star(t))^{-1} G(\theta^\star(t)) M \begin{pmatrix} F_1^\star(t) \\ F_2^\star(t) \end{pmatrix}$$

for all $t \in [t_0, t_f]$.

The control law for the TL dynamics (7) is then chosen as

$$F_\theta = -K_P(\theta - \theta^\star + K_D(\dot\theta - \dot\theta^\star)) + F_\theta^\star \tag{12}$$

with K_D, K_P positive design parameters. It turns out that K_D and K_P can be tuned so that the closed-loop trajectory tracks, with an error bounded by ϵ, the reference maneuver provided that initial error and the uncertainty on μ are sufficiently small. This is detailed in the next proposition (whose proof is deferred in Appendix A) in which we let $u = (F_1, F_2)$ and $\xi = (\theta, \dot\theta)$.

Proposition 1: Consider the closed-loop system resulting from (7) and (12). Let $K_D > 0$. There exists a $K_P^\star > 0$ such that for all $K_P \geq K_P^\star$ there exist $\Delta_{TL,0} > 0$ and $\Delta_{TL,\mu} > 0$ such that if $\|\xi(t_0) - \xi^\star(t_0)\| < \Delta_{TL,0}$ and $\|\mu - \mu_0\| \leq \Delta_{TL,\mu}$ the following holds

$$\|(\xi(t) - \xi^\star(t), u(t) - u^\star(t))\| < \epsilon \qquad \forall\, t \in [t_0, t_f]\,.$$

3) Low level controller in the TLs mode: With $u^\star(t) = (F_1^\star(t), F_2^\star(t)) : [t_0, t_f] \to \mathbb{R}^2$ and $\xi^\star(t) = (\alpha^\star(t), \dot\alpha^\star(t), \theta^\star(t), \dot\theta^\star(t)) : [t_0, t_f] \to \mathbb{R}^4$ a robust reference maneuver solution of the optimal problem in Section IV-B, for some $\epsilon > 0$ and using the dynamics (4), we define (see (3))

$$\begin{pmatrix} F_\alpha^\star(t) \\ F_\theta^\star(t) \end{pmatrix} = L(\theta^\star(t))^{-1} G(\theta^\star(t)) M \begin{pmatrix} F_1^\star(t) \\ F_2^\star(t) \end{pmatrix}$$

for all $t \in [t_0, t_f]$.

The control law for the TLs dynamics (4) is then chosen as

$$\begin{array}{rcl} F_\alpha &=& -K_P(\alpha - \alpha^\star + K_D(\dot\alpha - \dot\alpha^\star)) + F_\alpha^\star \\ F_\theta &=& -K_P(\theta - \theta^\star + K_D(\dot\theta - \dot\theta^\star)) + F_\theta^\star \end{array} \tag{13}$$

with K_D, K_P positive design parameters. The main properties of the closed-loop system are detailed in the next proposition in which it is show how, for an appropriate tuning of K_D and K_P, the actual closed-loop trajectory remains ϵ-close to the robust reference maneuver provided that the initial condition is sufficiently close to the reference and the uncertainty on μ is sufficiently small. In the statement of the proposition we let $u = (F_1, F_2)$ and $\xi = (\alpha, \dot\alpha, \theta, \dot\theta)$.

Proposition 2: Consider the closed-loop system (4) and (13). There exist a $K_D^\star > 0$ and, for all positive $K_D \leq K_D^\star$, a $K_P^\star > 0$ such that for all $K_D \leq K_D^\star$ and $K_P \geq K_P^\star$ there exist $\Delta_{TLs,0} > 0$ and $\Delta_{TLs,\mu} > 0$ such that if $\|\xi(t_0) - \xi^\star(t_0)\| < \Delta_{TLs,0}$ and $\|\mu - \mu_0\| \leq \Delta_{TLs,\mu}$ the following holds

$$\|(\xi(t) - \xi^\star(t), u(t) - u^\star(t))\| < \epsilon \qquad \forall\, t \in [t_0, t_f]\,.$$

The proof of the proposition is deferred in Appendix B.

4) Control in Free Flight: Let $u^\star(t) = (F_1^\star(t), F_2^\star(t)) : [t_0, t_f] \to \mathbb{R}^2$ and $\xi^\star(t) = (z^\star(t), \dot z^\star(t), x^\star(t), \dot x^\star(t), \theta^\star(t), \dot\theta^\star(t)) : [t_0, t_f] \to \mathbb{R}^6$ a robust reference maneuver solution of the optimal problem in Section IV-B for some $\epsilon > 0$ and using the free flight operative mode dynamics (2). The control law governing the quadrotor is free-flight is chosen as follow

$$\begin{pmatrix} F_1 \\ F_2 \end{pmatrix} = \frac{1}{2} \begin{pmatrix} \frac{1}{\cos\theta} & 1 \\ \frac{1}{\cos\theta} & -1 \end{pmatrix} \begin{pmatrix} u_1 + (F_1^\star + F_2^\star)\cos\theta^\star \\ u_2 + F_1^\star - F_2^\star \end{pmatrix} \tag{14}$$

where

$$\begin{array}{rcl} u_1 &=& -k_1(z - z^\star) - k_2(\dot z - \dot z^\star) \\ u_2 &=& -K_P(K_D(\dot\theta - \dot\theta^\star) + \tan\theta - \tan\theta^\star + \theta_{\text{out}}) \end{array}$$

and

$$\theta_{\text{out}} = \lambda_2 \sigma\left(\frac{K_2}{\lambda_2}\zeta\right), \quad \zeta = \dot x - \dot x^\star + \lambda_1 \sigma\left(\frac{K_1}{\lambda_1}(x - x^\star)\right) \tag{15}$$

where K_D, K_P, k_i, λ_i, K_i, with $i = \{1, 2\}$, are positive design parameters and $\sigma(\cdot)$ is a saturation function. The proposed control structure rests upon the design idea proposed in [18] and can be interpreted as a cascade control structure constituted by an inner loop, controlling the angular $(\theta, \dot\theta)$ dynamics, and an outer loop governing the lateral $(x, \dot x)$ and vertical $(z, \dot z)$ dynamics. The next proposition details the tuning of the previous controller in order to achieve the desired asymptotic properties. In the statement of the proposition we let $u = (F_1, F_2)$, $\xi = (z, \dot z, x, \dot x, \theta, \dot\theta)$. Furthermore, the tuning of the controller is given in terms of two parameters u^L and u^U defined as

$$u^L := \min_{t \in [t_0, t_f]} (F_1^\star(t) + F_2^\star(t))\cos\theta^\star(t)\,, \qquad u^U := 2F_{\max}\,.$$

For a proof, we refer the reader to [18] (see also [19]).

Proposition 3: Consider the closed-loop system given by (2) and (14)-(15) where δ_x and δ_z are exogenous bounded disturbances. Let k_1, k_2 be positive parameters and let λ_i, K_i be chosen as $\lambda_i = \varepsilon^{i-1}\lambda_i^\star$, $K_i = \varepsilon K_i^\star$, $i = 1, 2$, where ε is a design parameter and $(\lambda_i^\star, K_i^\star)$ satisfy

$$\frac{\lambda_2^\star}{K_2^\star} < \frac{\lambda_1^\star}{4}, \quad 8K_1^\star\lambda_1^\star < u_L\lambda_2^\star, \quad 24\frac{K_1^\star}{K_2^\star} < \frac{1}{6}\frac{u_L}{u_U}\,.$$

There exist $K_D^\star > 0$, $K_P^\star(K_D) > 0$ and $\varepsilon^\star(K_P) > 0$ such that for any positive $K_D < K_D^\star$, $K_P \geq K_P^\star(K_D)$ and $\varepsilon \leq \varepsilon^\star(K_P)$ there exist $\Delta_{FF,0} > 0$ and $\Delta_{FF,d} > 0$ such that if $\|\xi(t_0) - \xi^\star(t_0)\| \leq \Delta_{FF,0}$ and $\|(\delta_x, \delta_z)\|_\infty \leq \Delta_{FF,d}$ the following holds

$$\|(\xi(t) - \xi^\star(t), u(t) - u^\star(t)\| < \epsilon \qquad \forall\, t \in [t_0, t_f]\,.$$

D. Supervisor Design

With the definition of robust reference maneuvers and the properties of the low-level controllers highlighted above, the design of the supervisor reduces to orchestrate the switch of the low-level controllers and drive them with the appropriate reference maneuver according to the actual state of the vehicle. Specifically, we assume that four robust reference maneuvers $(\xi_{LL}^\star, u_{LL}^\star) : [t_{01}, t_{f1}] \to \mathcal{D}(LL)$, $(\xi_{TL}^\star, u_{TL}^\star) : [t_{02}, t_{f2}] \to \mathcal{D}(TL)$, $(\xi_{TLs}^\star, u_{TLs}^\star) : [t_{03}, t_{f3}] \to \mathcal{D}(TLs)$, $(\xi_{FF}^\star, u_{FF}^\star) : [t_{04}, t_{f4}] \to \mathcal{D}(FF)$ are given as solutions of the optimal problem developed in Section IV-B for some fixed ϵ and respective operative mode. Furthermore, with the reference maneuvers and ϵ fixed, we fix the four low-level controllers according to the structures and the design principles specified in Section IV-C. Specifically, we let u_{LL}, u_{TL}, u_{TLs}, u_{FF} be the control laws designed respectively in (11), (12), (13) and (14)-(15)

The supervisor logic switches the low-level controller according to the actual state $q(t)$ of the vehicle. The latter takes value in the set $\{LL, TL, TLs, FF\}$ and it is supposed to be known by the reading of sensors appropriately placed in the quadrotor airframe. The supervisor logic is thus simply $u(t) = u_{q(t)}(t)$. In the next items we detail the main properties achieved by the resulting closed-loop system that show how the desired take-off maneuver takes place. The claims in the items come immediately by joining the notion of robust reference maneuver and the properties of the low-level controllers highlighted in the Propositions in Section IV-C.

- Let $F_1(t_{01})$, $F_2(t_{02})$ be fulfilling the initial state restriction in the landed operative mode. Then there exists a time $t_{s1} \leq t_{f1}$ such that $q(t) = LL$ for all $t \in [t_{01}, t_{s1})$ and $q(t_{s1}) = TL$. At time t_{s1} the low-level controller is thus switched to u_{TL}.

- Let the uncertainties on the friction value be fulfilling $|\mu - \mu_0| \leq \Delta_{TL,\mu}$ with $\Delta_{TL,\mu}$ coming from Proposition 1. Then there exists a time $t_{s2} \leq t_{s1} + t_{f2} - t_{02}$ such that $q(t) = TL$ for all $t \in [t_{s1}, t_{s2})$ and $q(t_{s2}) = TLs$. At time t_{s2} the low-level controller is thus switched to u_{TLs}.
- Let the uncertainties on the friction value be fulfilling $|\mu - \mu_0| \leq \Delta_{TLs,\mu}$ and let $\xi^\star(t_{03})$ and $\xi(t_{s2})$ be such that $\|\xi(t_{s2}) - \xi^\star(t_{03})\| \leq \Delta_{TLs,0}$ with $\Delta_{TLs,\mu}$ and $\Delta_{TLs,0}$ introduced in Proposition 2. Then there exists a time $t_{s3} \leq t_{s2} + t_{f3} - t_{03}$ such that $q(t) = TLs$ for all $t \in [t_{s2}, t_{s3})$ and $q(t_{s3}) = FF$. At time t_{s3} the low-level controller is thus switched to u_{FF}.
- Let the exogenous disturbances (δ_x, δ_z) be fulfilling $\|(\delta_x, \delta_z)\|_\infty \leq \Delta_{FF,d}$ and let $\xi^\star(t_{04})$ and $\xi(t_{s3})$ be such that $\|\xi(t_{s3}) - \xi^\star(t_{04})\| \leq \Delta_{FF,0}$ with $\Delta_{FF,d}$ and $\Delta_{FF,0}$ introduced in Proposition 3. Then for all $t \in [t_{s3}, t_{s3} + t_{f4} - t_{04}]$ the vehicle evolves robustly in free-flight by tracking the reference maneuver with an error upper bounded by ϵ.

V. Simulation Results

In this section we present the results from a simulation run of the proposed controller conducted using a software simulator for hybrid systems [8]. To compute the reference maneuvers as solutions to the constrained optimal control problems formulated in Section IV-B, a numerical tool, named DIDO, has been adopted. DIDO implements a *direct collocation method* (see for example [20] for an overview of numerical optimization techniques) based upon Legendre pseudo-spectral (PS) approximation. A detailed description of the tool can be found in [21]. The numerical optimization process of DIDO can be controlled by setting the number of node points. Limiting to 20 the maximum number of nodes employed to generate the maneuvers used in the simulations, obtaining in few seconds feasible suboptimal solutions to be used directly as references.

The vehicle and terrain parameters are $m = 1$ kg, $J = 0.5$ kg m^2, $l_g = 0.3$ m, $\gamma = 30°$, $r = 0.5$ m, $\beta = 0.2$ rad, $\mu = 0.45$, and $\mu_0 = 0.5$. The controller design parameters are $K_P = 3$, $K_D = 3$ for the TL and TLs modes local controllers and $K_D = 0.3$, $K_P = 70$ for the FF controller. To attest the robustness of the proposed controller to sensor noise, the measurements of the states have been corrupted with additive gaussian white noise of zero mean and standard deviation of 0.02 m, 0.02 m/s, 1.14° and 1.14°/s. The vertical bars overimposed on the figures denote the time instants when a transition of hybrid state occurs.

For the take-off procedure, the reference trajectory consists of a sequence of robust approach maneuvers LL→TL, TL→TLs, and TLs→FF, resulting in the vehicle sliding up the slope. This maneuver is chosen in contrast with the situation presented in Figure 1, where the application of a heuristic take-off procedure results in the quadrotor sliding down the slope and hitting an obstacle.

The time evolution of the system's states and actuations are presented in Figure 6. The discontinuities that arise in the forces and the reference trajectories are due to the fact that the initial conditions for the new transition maneuver do not necessarily correspond to the end conditions of the approach maneuver leading into it. The final discrepancy between the desired and the actual trajectory is due to an imperfect knowledge of the friction coefficient μ. As a consequence, practical tracking of the trajectories is achieved, with an error smaller than ϵ, and the maneuver culminates with a successful robust transition to the free flight operative mode.

VI. Conclusions

This paper addressed the problem of robust take-off control of a quadrotor UAV, considering explicitly the interaction with the ground,

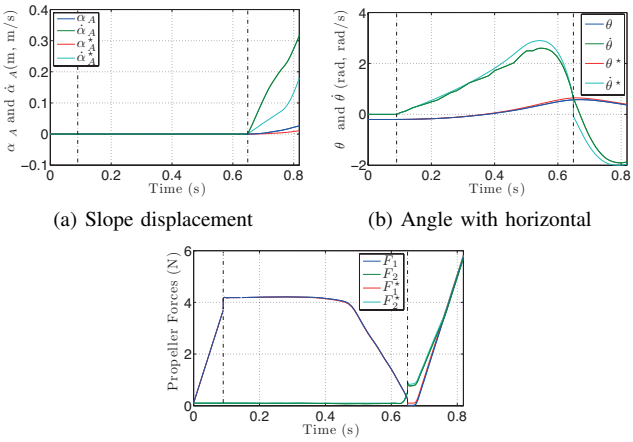

(a) Slope displacement (b) Angle with horizontal

(c) Actuations

Fig. 6. Comparison of the simulation maneuver and the desired maneuver for the quadrotor take-off.

that guarantees successful maneuvers even in sloped terrains and in the presence of external disturbances and uncertain parameters. The vehicle was modeled as a hybrid automaton, whose states reflect the different dynamic behaviors exhibited by the UAV. The take-off procedure was then cast as the problem of changing the operating mode from the initial to the final desired state, through the edges allowed for the hybrid automaton. The transitions between intermediate operating modes were achieved through the application of low-level feedback controllers, associated with each mode, to track robust reference signals. The supervisor and the combined properties of the low-level controllers and reference trajectories ensures that the desired intermediate transitions are attained, robustly to with respect to uncertainties in the model and environment parameters, and that the final desired state is reached.

Simulation results were presented to assess the performance of the proposed hybrid controller, demonstrating the effectiveness of the proposed solution, especially for the cases in which the slope of the terrain renders the take-off maneuvers more critical to be achieved.

Future works will be primarily focused on the experimental validation of the proposed solution for the take-off problem, as well as improvements to the hybrid dynamical model and the hybrid controller. In particular, for the experimental activity, a complex integration of the sensors (contact, force) and all the avionics equipments will be required, extending the standard sensing capabilities of the vehicle in order to robustly detect the current operative mode. This latter issue suggests also to investigate methodological solutions aiming at improving robustness to the possible uncertainties that may affect the measure of the current hybrid state. Another interesting research topic is the appropriate extension of the proposed framework to a third dimension, by adapting the presented arguments, allowing the controller to handle more complex scenarios in terms of the characteristics of the possible environment of operation.

References

[1] "Civilian applications: the challenges facing the uav industry," *Air & Space Europe*, 1999.

[2] T. Samad, J. Bay, and D. Godbole, "Network-centric systems for military operations in urban terrain: The role of uavs," *Proceedings of the IEEE*, vol. 95, no. 1, pp. 92–107, Jan. 2007.

[3] K. Ro, J.-S. Oh, and L. Dong, "Lessons learned: Application of small uav for urban highway traffic monitoring," *45th AIAA Aerospace Sciences Meeting and Exhibit*, 2007.

[4] J. M. Sullivan, "Revolution or evolution? the rise of the uavs," *45th AIAA Aerospace Sciences Meeting and Exhibit*, 2007.

[5] J. F. Roberts, T. S. Stirling, J.-C. Zufferey, and D. Floreano, "Quadrotor using minimal sensing for autonomous indoor flight," in *7th European Micro Air Vehicle conference and flight competition*, 2007.
[6] S. Bouabdallah and R. Siegwart, "Full control of a quadrotor," in *Intelligent Robots and Systems, 2007. IROS 2007. IEEE/RSJ International Conference on*, 29 2007-nov. 2 2007, pp. 153 –158.
[7] R. Mahony and T. Hamel, "Adaptive compensation of aerodynamic effects during takeoff and landing maneuvers for a scale model autonomous helicopter," *European Journal of Control*, vol. 7, no. 3, pp. 43 – 58, 2001.
[8] R. Goebel, R. Sanfelice, and A. Teel, "Hybrid dynamical systems," *Control Systems Magazine, IEEE*, vol. 29, no. 2, pp. 28–93, April 2009.
[9] T. J. Koo, F. Hoffmann, F. H. Mann, H. Shim, B. Sinopoli, and S. Sastry, "Hybrid control of an autonomous helicopter," in *In IFAC Workshop on Motion Control*, 1998, pp. 285–290.
[10] E. Frazzoli, M. Dahleh, and E. Feron, "A hybrid control architecture for aggressive maneuvering of autonomous helicopters," in *Decision and Control, 1999. Proceedings of the 38th IEEE Conference on*, vol. 3, 1999, pp. 2471 –2476.
[11] L. Marconi, R. Naldi, and L. Gentili, "A control framework for robust practical tracking of hybrid automata," *Conference on Decision and Control*, 2009.
[12] R. Naldi, L. Marconi, and L. Gentili, "Robust takeoff and landing for a class of aerial robots," *Conference on Decision and Control*, 2009.
[13] L. Marconi, R. Naldi, and L. Gentili, "Modeling and control of a flying robot interacting with the environment," *Automatica*, vol. 47, pp. 2571–2583, 2011.
[14] E. Frazzoli, M. Dahleh, and E. Feron, "Maneuver-based motion planning for nonlinear systems with symmetries," *Robotics, IEEE Transactions on*, vol. 21, no. 6, pp. 1077 – 1091, dec. 2005.
[15] R. Sanfelice and E. Frazzoli, "A hybrid control framework for robust maneuver-based motion planning," in *American Control Conference, 2008*, june 2008, pp. 2254 –2259.
[16] A. Isidori, *Nonlinear Control Systems II*. Springer Verlag London, 1999.
[17] A. Harnoy, B. Friedland, and S. Cohn, "Modeling and measuring friction effects," *Control Systems Magazine, IEEE*, vol. 28, no. 6, pp. 82 –91, dec. 2008.
[18] A. Isidori, L. Marconi, and A. Serrani, *Robust Autonomous Guidance*. Springer, 2003.
[19] L. Marconi and R. Naldi, "Robust full degree-of-freedom tracking control of a helicopter," *Automatica*, vol. 43, no. 11, pp. 1909 – 1920, 2007.
[20] J. Betts, *Practical Methods for Optimal Control Using Nonlinear Programming*. SIAM, 2001.
[21] I. Ross, "A matlab application package for solving optimal control problems," Naval Postgraduate School, Monterey ,CA, USA, 2004.

APPENDIX

A. Proof of Proposition 1

With $\tilde{\theta}(t) = \theta(t) - \theta^\star(t)$ the closed-loop error dynamics can be written as

$$\ddot{\tilde{\theta}} = -K_P(\tilde{\theta} + K_D\dot{\tilde{\theta}}) + \Psi_\theta(\tilde{\theta}, \dot{\tilde{\theta}}),$$

where

$$\Psi_\theta(\tilde{\theta}, \dot{\tilde{\theta}}) = h_\theta(\theta^\star + \tilde{\theta}, \dot{\theta}^\star + \dot{\tilde{\theta}}, 0, \mu) - h_\theta(\theta^\star, \dot{\theta}^\star, 0, \mu),$$

with $h_\theta(\cdot)$ defined in (6). Form this the result immediately follows by using the fact that $\Psi_\theta(\cdot,\cdot)$ is locally Lipschitz and the definition of u.

B. Proof of Proposition 2

Let $\tilde{\theta} := \theta - \theta^\star$ and $\tilde{\alpha} := \alpha - \alpha^\star$, and note that (4) in the new coordinates transform as

$$\ddot{\tilde{\theta}} = \tilde{F}_\theta + \Psi_\theta(\tilde{\theta}, \dot{\tilde{\theta}}, \dot{\tilde{\alpha}}, t) + \delta_\theta(t)\,, \quad \ddot{\tilde{\alpha}} = \tilde{F}_\alpha + \Psi_\alpha(\tilde{\theta}, \dot{\tilde{\theta}}, \dot{\tilde{\alpha}}, t) + \delta_\alpha(t)\,,$$

where (see (5) and (6))

$$\Psi_\theta(\tilde{\theta}, \dot{\tilde{\theta}}, \dot{\tilde{\alpha}}, t) = h_\theta(\theta^\star + \tilde{\theta}, \dot{\theta}^\star + \dot{\tilde{\theta}}, \dot{\alpha}^\star + \dot{\tilde{\alpha}}, \mu) - h_\theta(\theta^\star, \dot{\theta}^\star, \dot{\alpha}^\star, \mu)$$
$$\Psi_\alpha(\tilde{\theta}, \dot{\tilde{\theta}}, \dot{\tilde{\alpha}}, t) = h_\alpha(\theta^\star + \tilde{\theta}, \dot{\theta}^\star + \dot{\tilde{\theta}}, \dot{\alpha}^\star + \dot{\tilde{\alpha}}, \mu) - h_\alpha(\theta^\star, \dot{\theta}^\star, \dot{\alpha}^\star, \mu)$$
$$\delta_\theta(t) = (\mu - \mu_0)\frac{g\cos\beta\sin(\theta^\star + \gamma + \beta)}{\ell\cos(\theta^\star(t) + \gamma + \beta)^2}\mathrm{sgn}(\dot{\alpha}^\star(t))$$
$$\delta_\alpha(t) = -(\mu - \mu_0)\frac{g\cos\beta}{\cos(\theta^\star(t) + \gamma + \beta)^2}\mathrm{sgn}(\dot{\alpha}^\star(t))$$

and $\tilde{F}_\theta := F_\theta - F_\theta^\star$, $\tilde{F}_\alpha := F_\alpha - F_\alpha^\star$ with F_θ and F_α defined in (13). We observe that, by definition of $\theta^\star$, the functions $\delta_\alpha(t)$ and $\delta_\theta(t)$ satisfies $|\delta_\delta(t)| \le L_\delta|\mu - \mu_0|$ and $|\delta_\alpha(t)| \le L_\alpha|\mu - \mu_0|$ for all $t \ge 0$, for some positive constants L_δ and L_α.

Define the change of variables $\theta_1 := \tilde{\theta}$, $\theta_2 := \dot{\tilde{\theta}} + \frac{1}{K_D}\tilde{\theta}$, $\alpha_1 := \tilde{\alpha}$, $\alpha_2 := \dot{\tilde{\alpha}} + \frac{1}{K_D}\tilde{\alpha}$ which transforms the closed-loop error system into

$$\begin{aligned}\dot{\theta}_1 &= -\tfrac{1}{K_D}\theta_1 + \theta_2, \\ \dot{\theta}_2 &= -K_PK_D\theta_2 + \Psi_\theta(\theta_1, \theta_2 - \tfrac{1}{K_D}\theta_1, \alpha_2 - \tfrac{1}{K_D}\alpha_1, t) \\ &\quad - \tfrac{1}{K_D^2}\theta_1 + \tfrac{1}{K_D}\theta_2 + \delta_\theta,\end{aligned} \tag{16}$$

and

$$\begin{aligned}\dot{\alpha}_1 &= -\tfrac{1}{K_D}\alpha_1 + \alpha_2, \\ \dot{\alpha}_2 &= -K_PK_D\alpha_2 + \Psi_\alpha(\theta_1, \theta_2 - \tfrac{1}{K_D}\theta_1, \alpha_2 - \tfrac{1}{K_D}\alpha_1, t) \\ &\quad - \tfrac{1}{K_D^2}\alpha_1 + \tfrac{1}{K_D}\alpha_2 + \delta_\alpha.\end{aligned} \tag{17}$$

Let $\rho := \min_{t\in[t_0,t_f]}\theta^\star(t) + \beta$ and note that $\rho > \epsilon > 0$. Define the Lyapunov function $V(\theta_1,\theta_2,\alpha_1,\alpha_2) = V_\theta(\theta_1,\theta_2) + V_\alpha(\alpha_1,\alpha_2)$ where

$$V_\theta(\theta_1,\theta_2) := \frac{\theta_1^2}{\rho - |\theta_1|} + \frac{1}{2}\theta_2^2\,, \quad V_\alpha(\alpha_1,\alpha_2) := \frac{1}{2}\left(\alpha_1^2 + \alpha_2^2\right)\,,$$

and note that $V(\theta_1,\theta_2,\alpha_1,\alpha_2)$ is defined and radially unbounded on the domain $(-\rho,\rho)\times\mathbb{R}\times\mathbb{R}\times\mathbb{R}$. Furthermore, let $\Omega(\ell) := \{(\theta_1,\theta_2,\alpha_1,\alpha_2) \,:\, V \le \ell^2\}$, a level set of V.

By using the fact that $\Psi_\theta(\cdot)$ and $\Psi_\alpha(\cdot)$ are locally Lipschitz and vanishing in $\theta_1 = 0$, $\theta_2 - \frac{1}{K_D}\theta_1 = 0$, $\alpha_2 - \frac{1}{K_D}\alpha_1 = 0$, for any ℓ there exist positive L_1 and L_1 such that for all $(\theta_1,\theta_2,\alpha_1,\alpha_2) \in \Omega_\theta(\ell)$ the following hold

$$\begin{aligned}&|\Psi_\theta(\theta_1,\, \theta_2 - \tfrac{1}{K_D}\theta_1,\, \alpha_2 - \tfrac{1}{K_D}\alpha_1,\, t)| \le \\ &\qquad L_1(K_D)|\theta_1| + L_1(K_D)|\alpha_1| + L_2|\theta_2| + L_2|\alpha_2| \\ &|\Psi_\alpha(\theta_1,\, \theta_2 - \tfrac{1}{K_D}\theta_1,\, \alpha_2 - \tfrac{1}{K_D}\alpha_1,\, t)| \le \\ &\qquad L_1(K_D)|\theta_1| + L_1(K_D)|\alpha_1| + L_2|\theta_2| + L_2|\alpha_2|\,,\end{aligned}$$

for all $t \ge 0$.

The time derivative of V_θ and V_α along the solutions of (16)-(17), can be upper bounded as

$$\begin{aligned}\dot{V}_\theta \;\le\;& T(\theta)\left(-\tfrac{1}{K_D}\theta_1^2 + |\theta_1||\theta_2|\right) + (-K_PK_D + L_2 + \tfrac{1}{K_D})\theta_2^2 \\ &+(L_1(K_D) + \tfrac{1}{K_D^2})|\theta_1||\theta_2| + L_1(K_D)|\theta_2||\alpha_1| \\ &+L_2|\theta_2||\alpha_2| + |\theta_2||\delta_\theta|\end{aligned}$$

$$\begin{aligned}\dot{V}_\alpha \;\le\;& \left(-\tfrac{1}{K_D}\alpha_1 + \alpha_2\right) + (-K_PK_D + L_2 + \tfrac{1}{K_D})\alpha_2^2 \\ &+(L_1(K_D) + \tfrac{1}{K_D^2})|\alpha_1||\alpha_2| + L_2|\theta_2||\alpha_1| \\ &+L_1(K_D)|\theta_1||\alpha_2| + |\alpha_2||\delta_\alpha|\end{aligned}$$

where $T(\theta_1) = \left(2 + \theta_1^2/|\theta_1|\right)/\left(\rho - |\theta_1|\right)^2$. Note that $T(\theta_1) \ge 2/\rho^2$ for all $\theta_1 \in \mathbb{R}$. By completing the squares, it follows that for any ℓ and for any c there exists a $K_D^\star > 0$ and a $K_P^\star(K_D) > 0$ such that

for any positive $K_D \leq K_D^\star$ and $K_P \geq K_P^\star$ the following bound on $\dot{V}$ can be established

$$\dot{V} \leq -\gamma \|(\theta_1, \theta_2, \alpha_1, \alpha_2)\| + c\|(\delta_\theta, \delta_\alpha)\|$$

for all $(\theta_1, \theta_2, \alpha_1, \alpha_2) \in \Omega_\ell$, where γ is a positive constant. From this the result follows by standard Lyapunov arguments by using the definition of u, of $(\delta_\theta, \delta_\alpha)$ and by noting that for any ℓ and K_D there exist a $\Delta_{TLs,0}$ such that

$$\begin{aligned}\{(\theta_1, \theta_2, \alpha_1, \alpha_2) \in \mathbb{R} \times \mathbb{R} \times \mathbb{R} \times \mathbb{R} \ : \\ |\theta_1| \leq \Delta_{TLs,0}, \ \ |\theta_2 - \tfrac{1}{K_D}\theta_1| \leq \Delta_{TLs,0} \\ |\alpha_1| \leq \Delta_{TLs,0}, \ \ |\alpha_2 - \tfrac{1}{K_D}\alpha_1| \leq \Delta_{TLs,0}\} \subset \Omega(\ell)\,.\end{aligned}$$